



Research Article

Effect of the position of the hot source on mixed convection in a rectangular cavity

Tewfik SEREIR^{1*}, Abdelkrim MISSOUM², Brahim MEBARKI², Mohammed ELMIR²,
Mohamed DOUHA²

¹Mechanical Modeling and Experimentation Laboratory, Tahri Mohamed University, Bechar 08000, Algeria

²Energariid Lab oratory, Faculty of Technology, Tahri Mohamed University of Bechar, B.P.417, 08000, Bechar, Algeria

ARTICLE INFO

Article history

Received: 01 July 2021

Accepted: 24 November 2021

Keywords:

Numerical Heat Transfer;
Rectangular Enclosure; Mixed
Convection; Position of the Hot
Source; Cooling; Sinusoidal
Temperature; Finite Element
Methods

ABSTRACT

This work presents a study by numerical simulation of mixed convection in a rectangular cavity with a sinusoidal temperature imposed on the right vertical wall while the other wall on the left is kept at a cold temperature. The upper and lower walls are thermally insulated, the inlet and outlet ports are respectively located on the hot wall to the bottom and on the top to the left. The enclosure represents a practical system such as an air-cooled electronic device, the heat source represents a radiator or an electronic component located in three different positions towards the left side at the bottom, the center and towards the right side at the top in such an enclosure. All calculations are made for a range of Richardson number from 0 to 10 and Reynolds numbers from 50 to 200. The influence of Richardson number, the position of the heat source and the influence of amplitude and phase deviation of the temperature imposed on the Nusselt number on the hot surface is studied. The results are presented in the form of streamlines and isotherms graphs as well as the variation in maximum temperature and mean Nusselt number under different conditions. The numerical resolution of the governing equations is obtained using the software of Multiphysics Comsol based on the finite element method.

Cite this article as: Sereir T, Missoum A, Mebarki B, Elmir M, Douha M. Effect of the position of the hot source on mixed convection in a rectangular cavity. J Ther Eng 2022;8(4):1–13.

INTRODUCTION

Recently, the numerical analysis of mixed convection flow structure and thermal phenomena inside ventilated cavities has become the most extensive research subject for its functional importance and application as: production

oil, air heating-cooling mechanism, nuclear reactors, heat exchangers and others.

In general, several scientific researchers have studied flow dynamics and heat transfer in both two and

*Corresponding author.

*E-mail address: sereirtewfik@gmail.com

This paper was recommended for publication in revised form by Regional Editor Hasan Köten



three-dimensional [1]–[4] configurations in various geometric shapes [5]–[14]. Due to its high performance and limited energy demand, a study of laminar mixed convection cooling of a rectangular cavity with a constant source of heat flow was the subject of [15] to identify optimum location of inlet and outlet for better cooling efficiency. For various ventilation arrangements, free and forced convection was investigated in a rectangular enclosure with a source heated from below. S. Mekroussi and al. [16] studied by numerical simulation the mixed air convection (Pr=0.71) in a cavity with corrugated walls. The influence of several control parameters on the flow such as the Richardson number, amplitude ratio and phase difference have been considered. Taylor and al. [17] carried out an experimental study of mixed convection in a ventilated cavity subjected to a heat flux on the vertical wall. [18] For the fields of flow and temperature distributions, numerical results are recorded in a heated solid enclosed in a square cavity with several geometric configurations. [19] studied two-dimensional mixed convection inside a ventilated cavity with central solid circular heated horizontal conductor for different cylinder size (0-0.6) and also Richardson number $0 < Ri < 500$ using the finite element method.

As a result, the phenomenon inside the cavity with or without a cylinder depends on both the transfer diameter of the cylinder and the number Ri.

[20] and [21] analyzed two-dimensional mixed convection in enclosures with adiabatic walls with two cylinders heated inside for a different diameter and a constant distance between the two cylinders. [22] Using a finite element method, a computer survey was carried out on mixed convection in a square cavity, in a ventilated square enclosure with an inlet located on the left edge of the insulated vertical wall, where the exhaust port is attached to the top of the heated vertical surface, this study examined and explained the complicated relationship between buoyancy and the flow of force. [23] Study of heat transfer and mixed convection flow patterns driven by the cover in a trapezoidal cavity with sinusoidal temperature at the bottom wall. [24] The mixed convection driven by the cover with a sinusoidal temperature in the two side walls in a square cavity was studied. [25] studied the two-dimensional ventilated rectangular cavity for various inlets and outlets using the finite element method. [26] three-dimensional mixed convection in a ventilated cavity for different locations of the inlet and outlet ports at various Reynolds and Richardson numbers.

The present work was carried out to study the heat transfer and the fluid patterns inside a rectangular enclosure in terms of the mean Nusselt number at the heated sinusoidal wall and the conductive square solid block inside the rectangular cavity for various parameters in order to achieve optimal mixed convection conditions. Finally, an empirical correlation equation is developed to calculate the mean Nusselt number.

DESCRIPTION OF THE PROBLEM

The studied physical system illustrated in Figure 1, consists of a rectangular cavity of width H and length L contains a square heat source of dimension d on each side. The two openings of dimension w, one of which is located in the right wall which serves for the outlet of hot air and the other for the inlet of cold air located in the upper wall.

The cavity is stressed by a hot temperature of the sinusoidal shape in the right vertical wall and the other left wall is kept at a cold temperature, so that both sides of the upper and lower part of the cavity are thermally insulated (adiabatic).

The simplifying assumptions are as follows:

- The flow is assumed to be two-dimensional and laminar
- The fluid is Newtonian
- The properties of fluid are constant
- The viscous dissipation and compressibility effects are considered negligible
- The heat exchange by radiation and the variations in density of the fluid are neglected except in the term of buoyancy.

In the fluid zone :

$$\frac{\partial U}{\partial X} + \frac{\partial V}{\partial Y} = 0 \quad (1)$$

$$U \frac{\partial U}{\partial X} + V \frac{\partial U}{\partial Y} = -\frac{\partial P}{\partial X} + \frac{1}{Re} \left(\frac{\partial^2 U}{\partial X^2} + \frac{\partial^2 U}{\partial Y^2} \right) \quad (2)$$

$$U \frac{\partial V}{\partial X} + V \frac{\partial V}{\partial Y} = -\frac{\partial P}{\partial Y} + \frac{1}{Re} \left(\frac{\partial^2 V}{\partial X^2} + \frac{\partial^2 V}{\partial Y^2} \right) + Ri\theta \quad (3)$$

$$U \frac{\partial \theta}{\partial X} + V \frac{\partial \theta}{\partial Y} = \frac{1}{Re.Pr} \left(\frac{\partial^2 \theta}{\partial X^2} + \frac{\partial^2 \theta}{\partial Y^2} \right) \quad (4)$$

In the solid zone :

$$\frac{\partial^2 \theta_s}{\partial X^2} + \frac{\partial^2 \theta_s}{\partial Y^2} = 0 \quad (5)$$

Dimensionless variables are defined as follows:

$$X = \frac{x}{H}, Y = \frac{y}{H}, U = \frac{u}{u_i}, V = \frac{v}{u_i}, P = \frac{p}{\rho u_i^2}, D = \frac{d}{H},$$

$$\theta = \frac{(T - T_i)}{(T_h - T_i)}, \lambda = \frac{\lambda_s}{\lambda_f}$$

The dimensionless numbers that appear in the previous equations are:

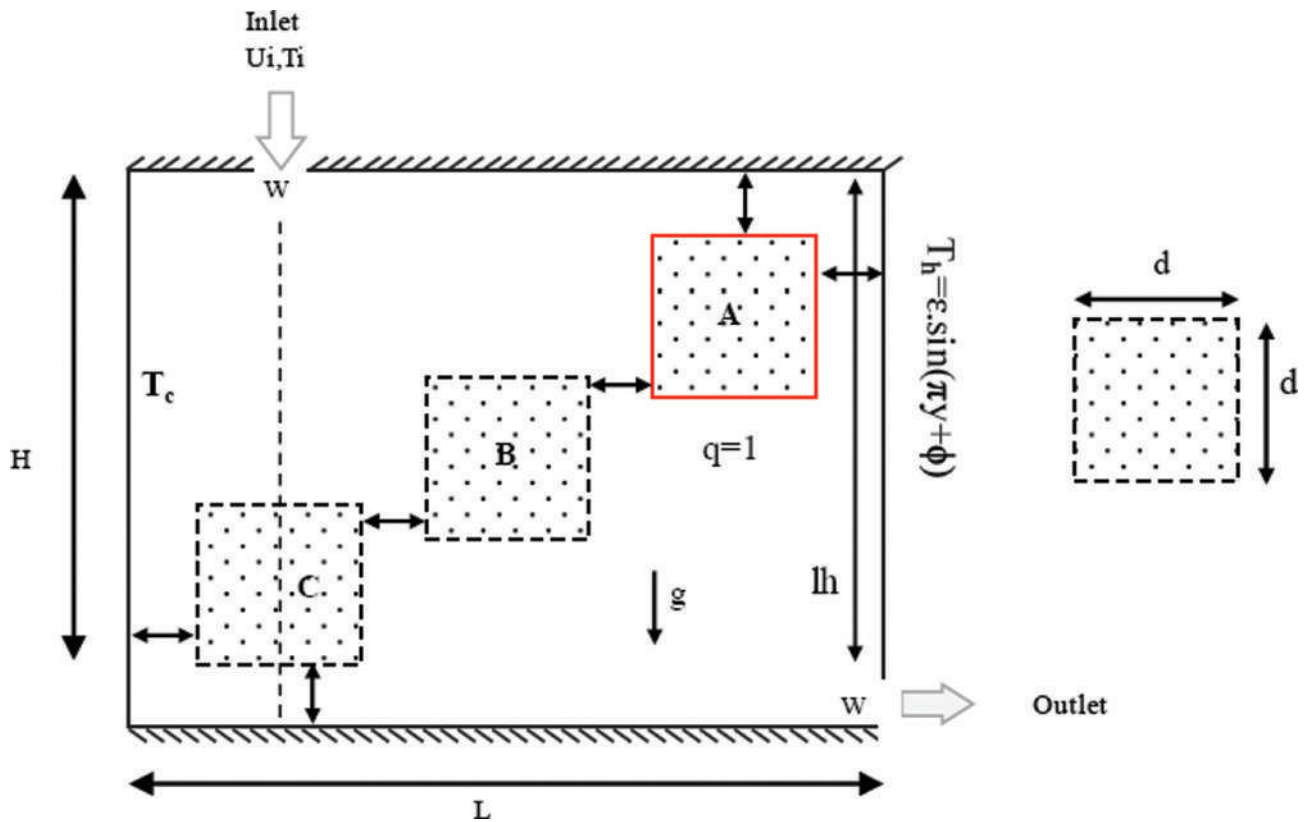


Figure 1. The physical model.

$$Pr = \frac{\nu}{\alpha}, Re = \frac{U_o H}{\nu}; Ri = \frac{Gr}{Re^2}, Gr = \frac{g\beta L^3 (T_h - T_i)}{\nu^2}$$

$$U = 0; V = 0 \text{ and } \frac{\partial \theta}{\partial Y} = 0$$

At the vertical solid-fluid interfaces:

$$\left(\frac{d\theta}{dX}\right)_{fluid} = \lambda \left(\frac{d\theta_s}{dX}\right)_{solid}$$

At the horizontal solid-fluid interfaces:

$$\left(\frac{d\theta}{dY}\right)_{fluid} = \lambda \left(\frac{d\theta_s}{dY}\right)_{solid}$$

Boundary condition

The boundary conditions of this analysis are:

- Lower horizontal wall :

$$U = 0; V = 0 \text{ and } \frac{\partial \theta}{\partial Y} = 0$$

- Left vertical wall :

$$\theta = 0, U = V = 0$$

At upper horizontal wall:

- At the entrance:

$$U = 0, V = -1 \text{ and } \theta = 0$$

At right vertical wall:

$$U = V = 0, \theta_h = \epsilon \cdot \sin(\pi Y + \phi),$$

- At the outlet:

convective boundary condition, (CBC), $P = 0$

$$\text{With } w = 0.1H, L = \frac{3}{2}H \text{ and } d = \frac{H}{3}$$

The average Nusselt number in vertical right wall and in the solid block of cavity is evaluated by:

- In the right vertical wall :

$$Nu = \frac{1}{L_h} \int_0^{L_h} Nu(Y) dY \tag{6}$$

- In the interface solid-fluid:

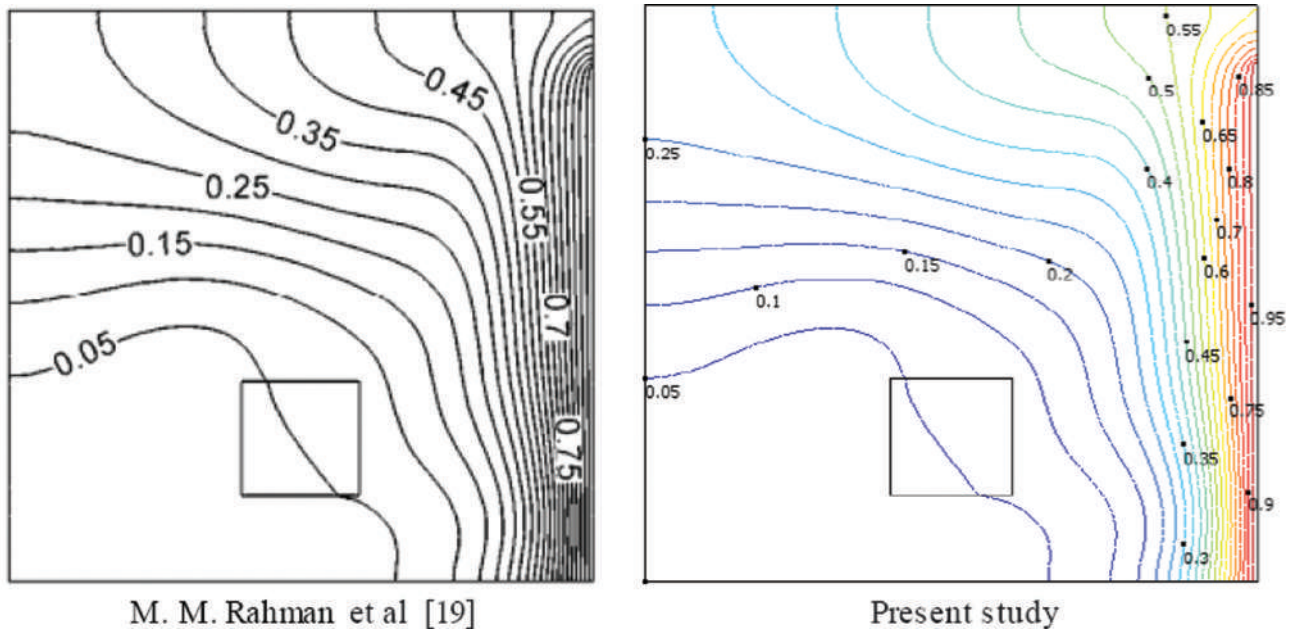


Figure 2. Isotherms for Ri = 5, Lx = 0.5, Ly = 0.25, λ = 0.5 and Re = 100.

According to Saha et al. [15] and in order to obtain a better value of the average Nusselt number, it is calculated from the average temperature and nom from the input temperature.

The average Nusselt number at the surface of the square solid is:

$$\begin{aligned}
 Nu_s &= \frac{1}{L_x} \int_0^{L_x} Nu(X) d\eta + \frac{1}{L_y} \int_0^{L_y} Nu(Y) d\eta \\
 &= \frac{1}{L_x} \int_0^{L_x} \frac{h \cdot X}{\lambda} dX + \frac{1}{L_y} \int_0^{L_y} \frac{h \cdot Y}{\lambda} dY
 \end{aligned}
 \tag{7}$$

In this case

$$h = \frac{q}{\theta - \theta_{av}}
 \tag{8}$$

The average temperature is defined as:

$$\theta_{av} = \frac{1}{V} \int \theta dV
 \tag{9}$$

Where V is the volume of the cavity.

NUMERICAL METHOD

The finite element method is used to resolve the governing equations. A direct linear system solver is adopted with a stationary nonlinear solver described by [27] and [28]. The relative tolerance for error is assumed to be 10⁻⁶ used with denser grids clustered in regions close to the heat source and enclosure walls.

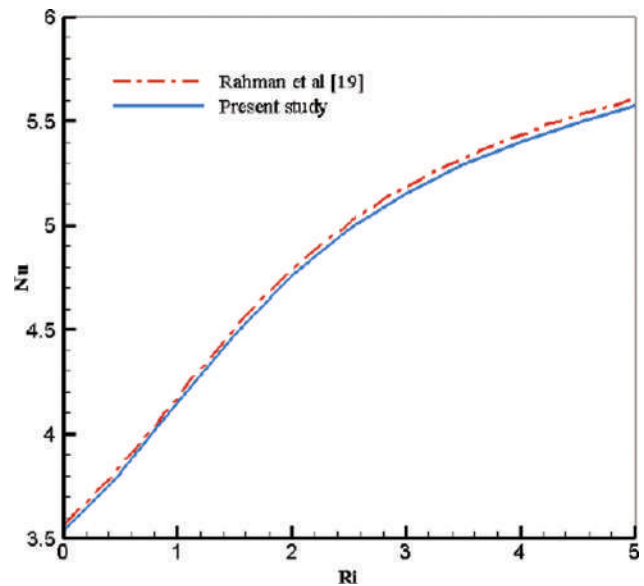


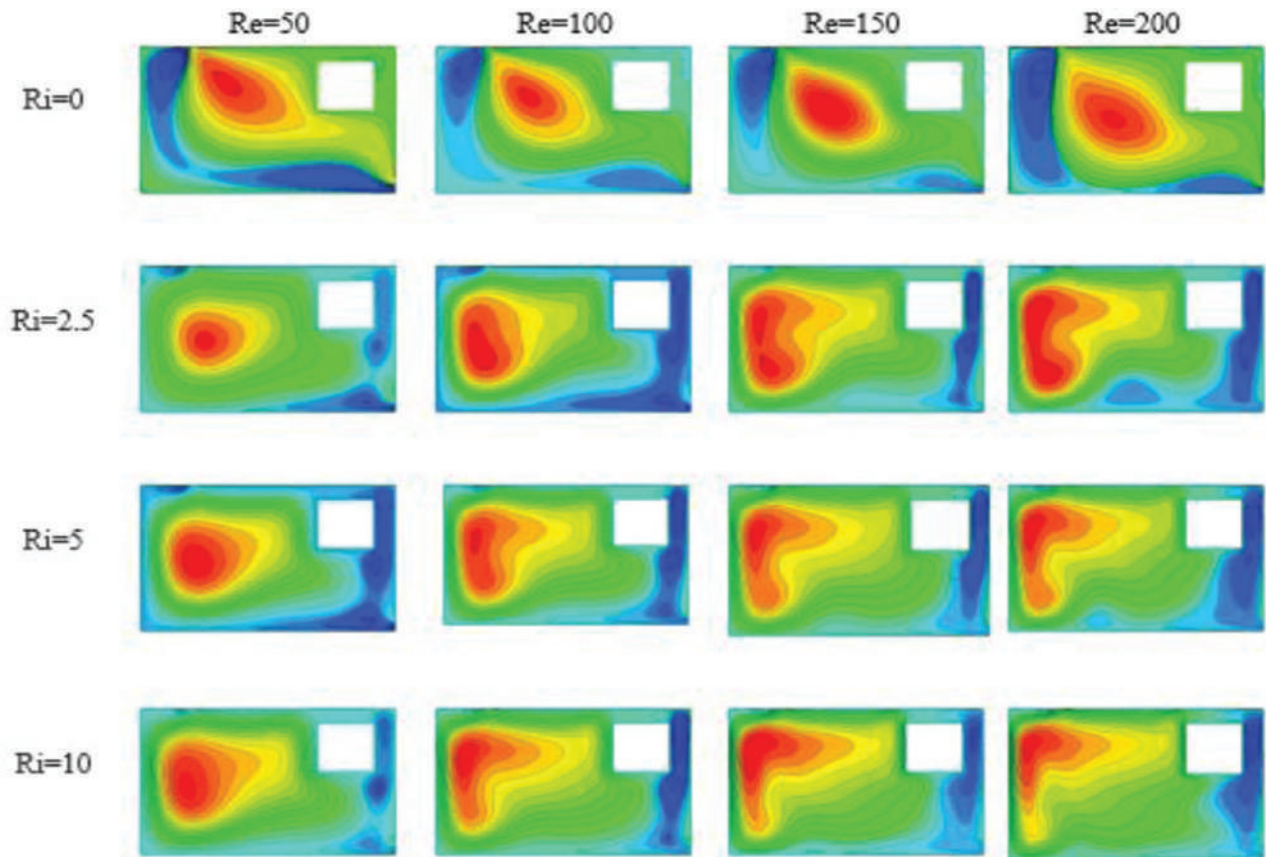
Figure 3. Average Nusselt Number for Lx = 0.5, Ly = 0.25, λ = 5, Re=100 between M. M. Rahman [19] and our work.

Our work has been validated with the work of Rahman et al [19]. We compared the isotherms and the average Nusselt number when the solid square was located at ly = lx = 0.5 with data from our results at Re = 100, Ri = 1.0, λ = 5.0 and lx = ly = 0.2. We found that the isotherms and the average Nusselt number agree well with those of Rahman et al, as shown in Figure 2 and Figure 3.

In this study, several grids sizes have been tested (8111, 8943, 9824, 10700, 11884 and 12236 elements) have been tested. The values of average Nusselt number are included

Table 1. Grid sensitivity Check at $Re=100$, $Ri=1.0$, $\lambda = 5$, $d=L/3$, $Lx=1.5/2$ and $Ly=0.5$

| Elements | 8111 | 8943 | 9824 | 10700 | 11884 | 12236 |
|----------|---------|---------|---------|---------|---------|---------|
| Nu | 47.5915 | 47.6468 | 47.6780 | 47.7272 | 47.7278 | 47.7280 |

**Figure 4.** The streamlines for a number of Ri from 0 to 10 and Re from 50 to 200 with an amplitude $\varepsilon = 1$, and a phase deviation $\varphi = 0$ for the “A” configuration.

in Table 1. The grid size 11884 elements is adopted since it provides more satisfaction results and less calculating time.

RESULTS AND DISCUSSION

Streamlines and isotherms

The current lines for a Richardson number from 0 to 10 and different Reynolds number from 50 to 200 with an amplitude of and a phase deviation of the configuration “A” are shown in Figure 4, In the case of forced convection $Ri = 0$, two small rotating vortices are formed near the left cold wall and the bottom wall of the cavity, respectively. As the Reynolds number increases, this vortex area becomes larger. As Ri increases, the rotating vortex becomes larger and the flow rate is strong near the horizontal cold wall and the appearance of a recirculation zone towards the side of the right hot wall. Increasing the Richardson number

increases the buoyancy effect and improves energy transport which leads to an increase in flow force.

Figure 5 represents the isotherms for a Richardson number from 0 to 10 and different Reynolds number from 50 to 200 with an amplitude of and a phase deviation of the configuration “A”, when the convection is forced ($Ri = 0$) the isotherms are more concentrated vertically around the heat source. Since the greatest amount of heat flow is removed from the source and dissipated through the outlet opening, hence the air flow from the inlet to the outlet to influence the heat transport and isotherms with high values tend to concentrate near the heat source so that the conduction mode of heat transfer dominates that of convection which is confirmed by layered isotherms.

The mixed convection regime becomes more noticeable with the increase in Ri because the energy transport increases due to the flow of conductive heat emitted by

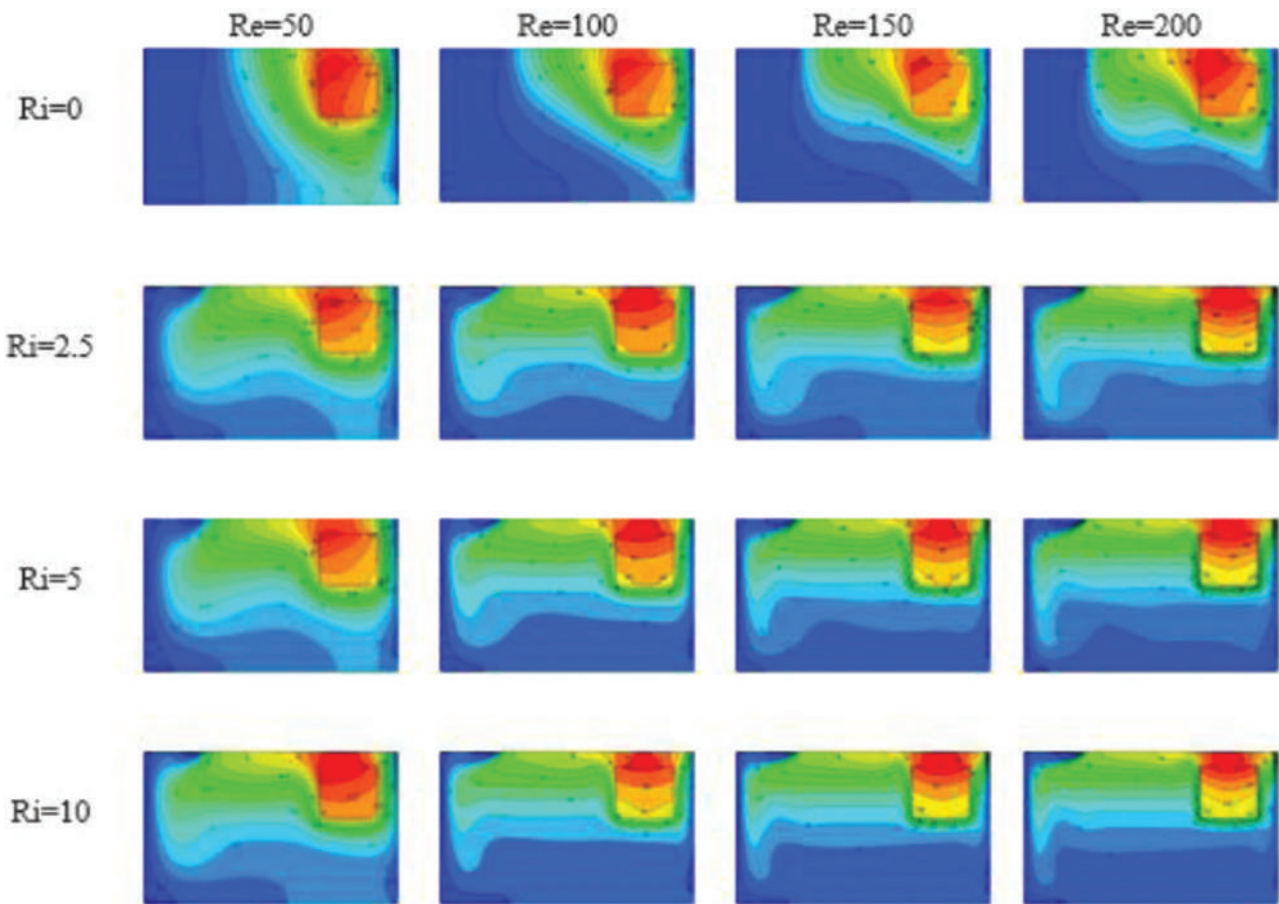


Figure 5. Isotherms for a number of Ri from 0 to 10 and Re from 50 to 200 with an amplitude of $\epsilon = 1$ and a phase-deviation of $\phi = 0$ for the configuration “A”.

the source. Since the isotherms change as Ri and Re vary, these are the concentration parameters in the analysis for all cases. Isotherms are more concentrated horizontally around the heat source and at the top of the cavity. When Re increases the isotherms are clustered near the heat source, because the induced fluid flows faster over the heat source, the heat conducted in the induced flow cannot propagate to the upper layers of the fluid.

The current lines of configuration “B” for a Richardson number from 0 to 10 and different Reynolds number from 50 to 200 with an amplitude of and a phase deviation are shown in Figure 6. hot source is in the center of the cavity the flow is symmetrical for $Ri > 0$ and becomes larger with the increase in the number of Re . In the case of forced convection $Ri = 0$ the appearance of two recirculation zones one is around the hot source and the second occurs from the inlet opening to the outlet port since the flow is faster than the flow dissipated by the hot source.

Figure 7 shows the isotherms for a Richardson number from 0 to 10 and different Reynolds number from 50 to 200 with an amplitude of and a phase deviation of the configuration “B”, in the case of forced convection the isotherms are

more concentrated. vertically near the hot source and as the number of Re increases, the isotherms near the cold wall and the fluid inlet become weaker than that of the source and the hot wall. On the other hand, the more Ri increases the isotherms are horizontal and always concentrated around the source since the heat flux is dominant than the flow flux.

The current lines of the configuration “C” for a Richardson number from 0 to 10 and different Reynolds number from 50 to 200 with an amplitude of and a phase deviation are illustrated in Figure 8 For $Ri = 0$ the appearance of two recirculation zone one of the air entering through the opening which circulates around the hot source to the outlet opening and the other vortex is located in the corner between the left hot wall and the part upper cavity. When the mixed convection $Ri > 0$ starts, two counter-rotating vortices, one of small size located above the hot source and near the cold air inlet opening and the other large size vortex occupies the rest of the cavity and as Re increases the flow is important.

The isotherms of the configuration “C” for a Richardson number from 0 to 10 and different Reynolds number from 50 to 200 with an amplitude of and a phase deviation are

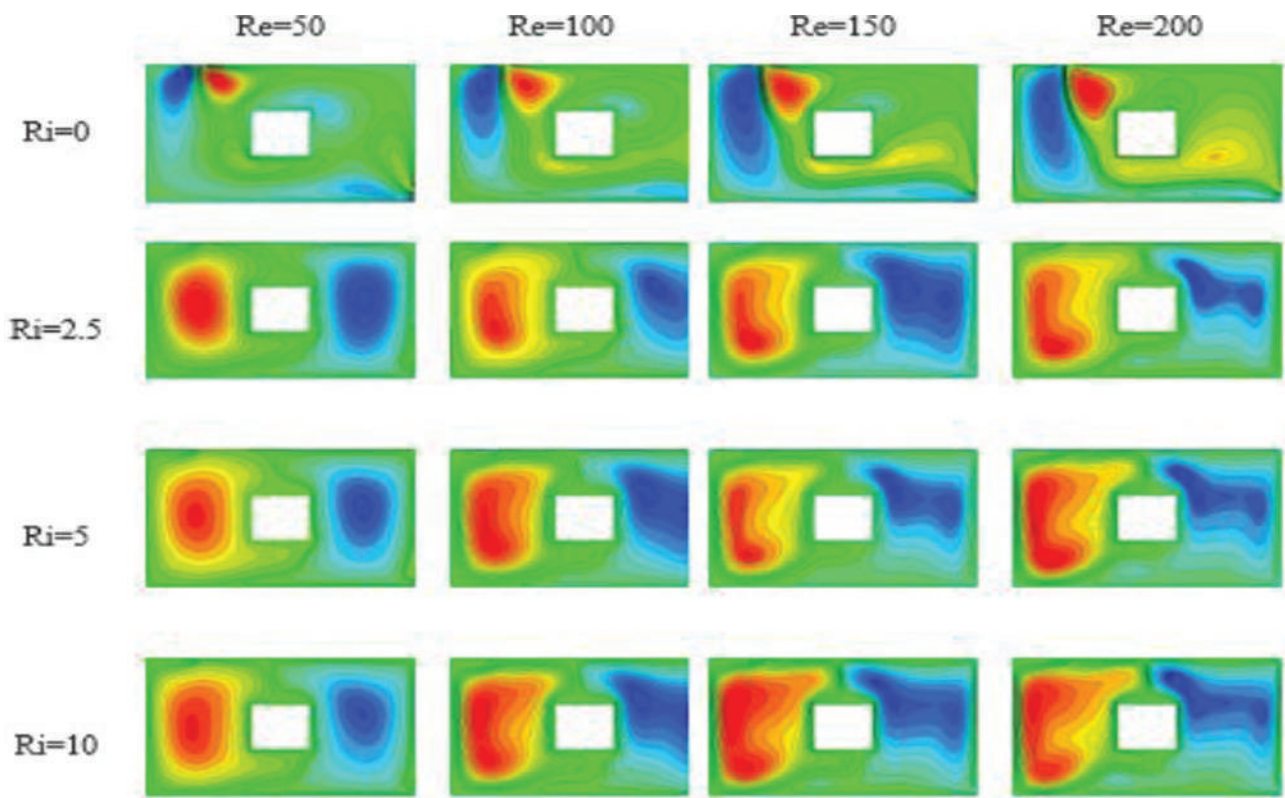


Figure 6. The streamlines for Ri from 0 to 10 and Re from 50 to 200 with an amplitude of $\varepsilon = 1$ and a phase-deviation of $\phi = 0$ for the configuration "B".

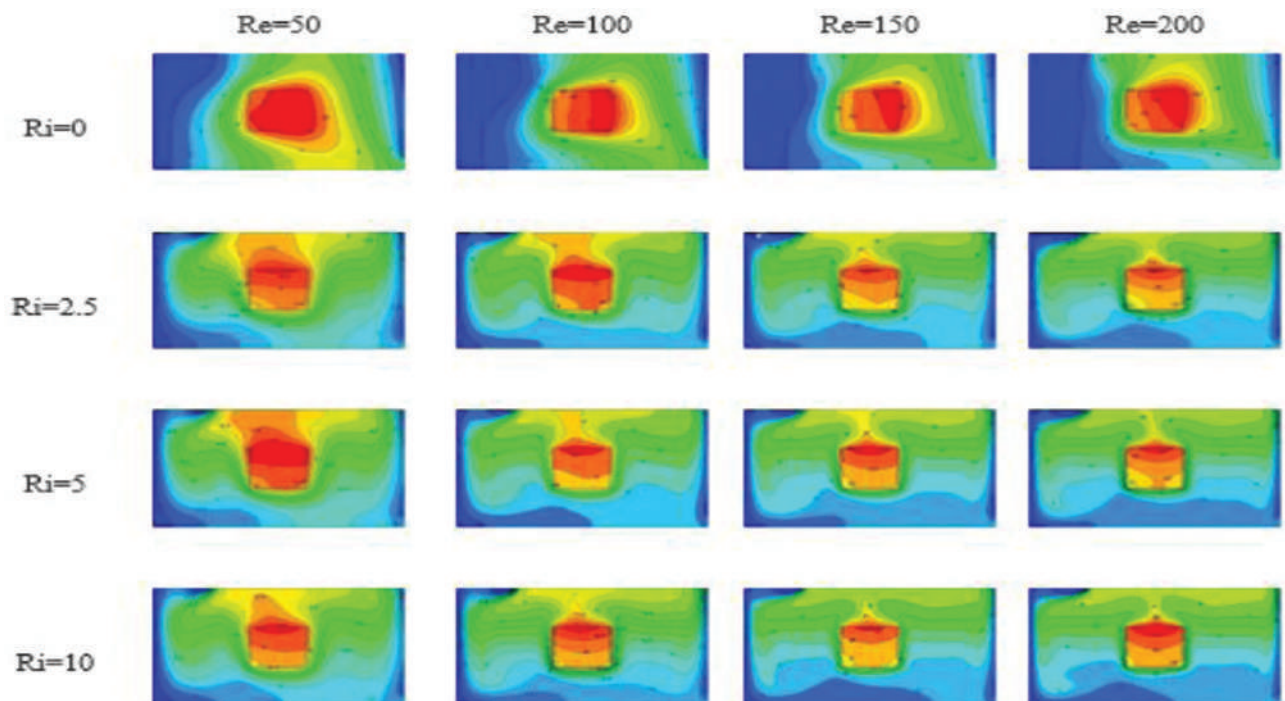


Figure 7. Isotherms for Ri from 0 to 10 and Re from 50 to 200 with an amplitude of $\varepsilon = 1$ and a phase-deviation of $\phi = 0$ configuration "B".

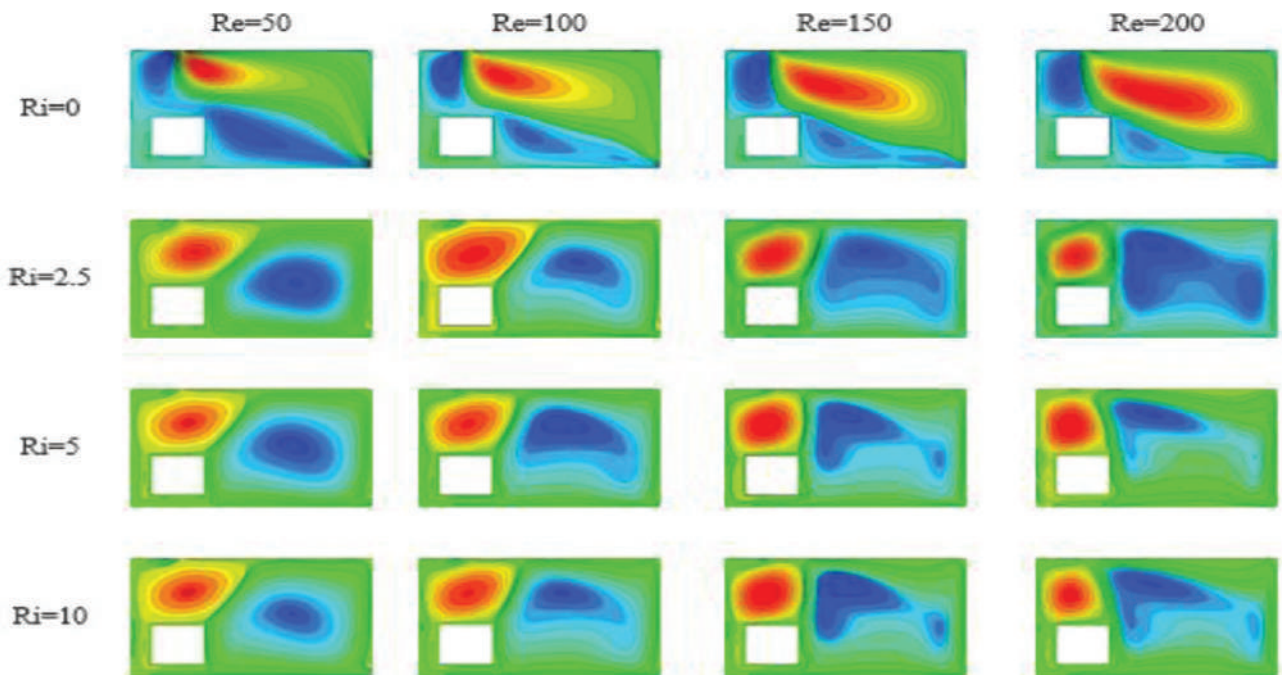


Figure 8. The current lines for Ri from 0 to 10 and Re from 50 to 200 with an amplitude of $\epsilon = 1$ and a phase deviation of $\phi = 0$ for the configuration “C”.

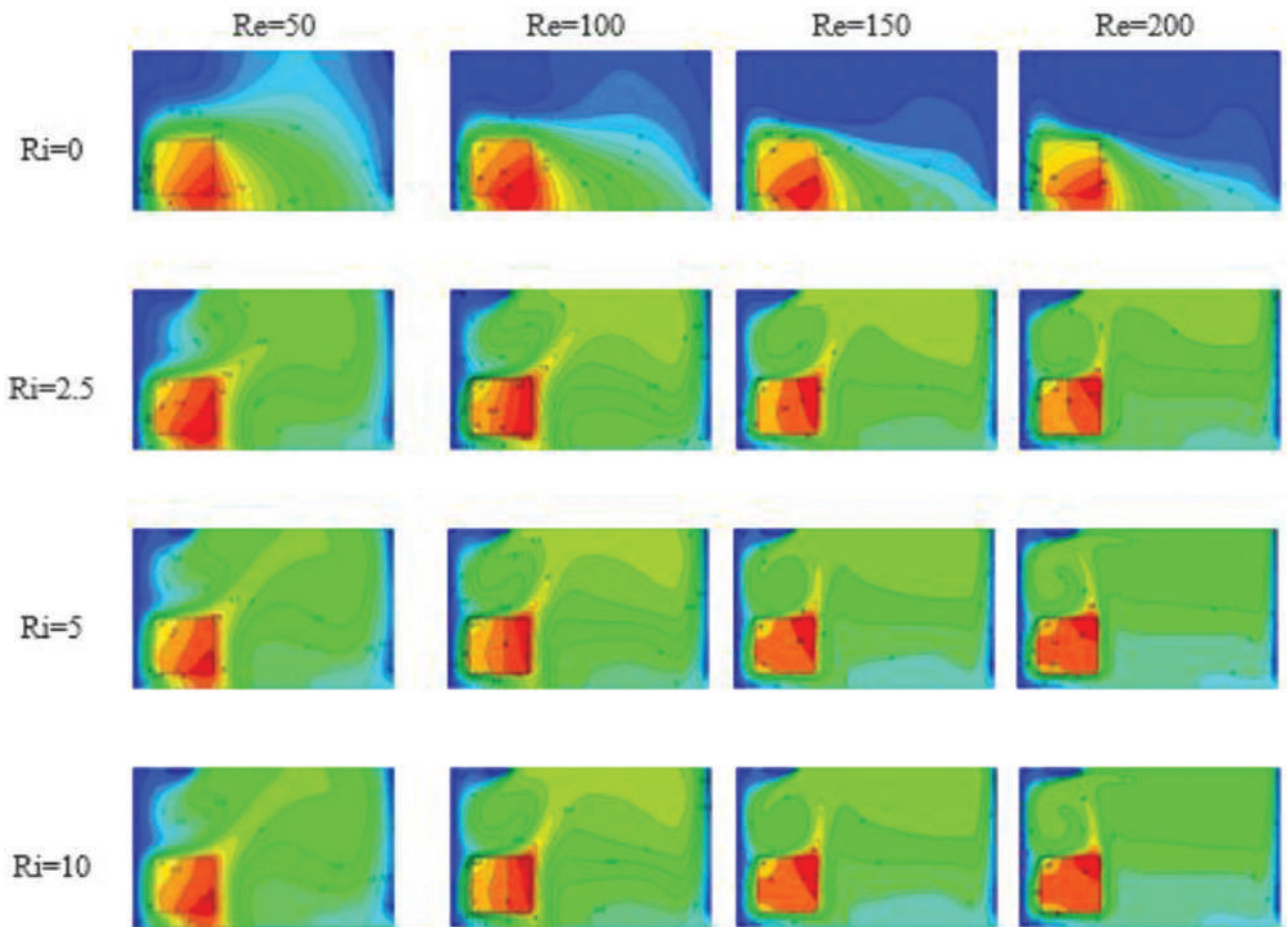


Figure 9. Isotherms for Ri from 0 to 10 and Re from 50 to 200 with an amplitude of $\epsilon = 1$ and a phase deviation of $\phi = 0$ for the configuration “C”.

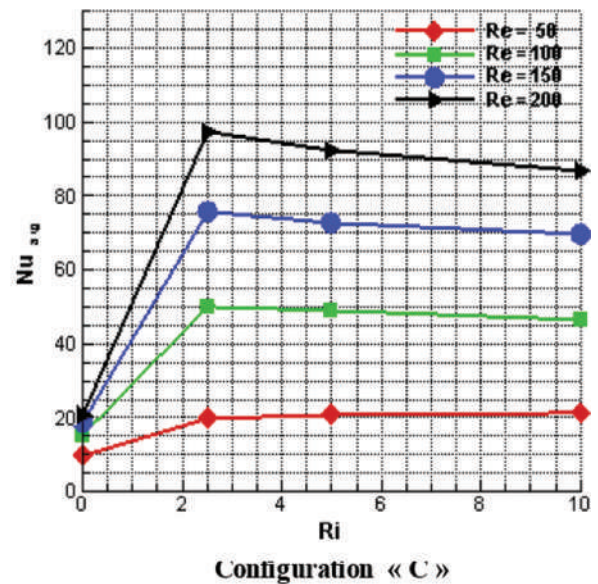
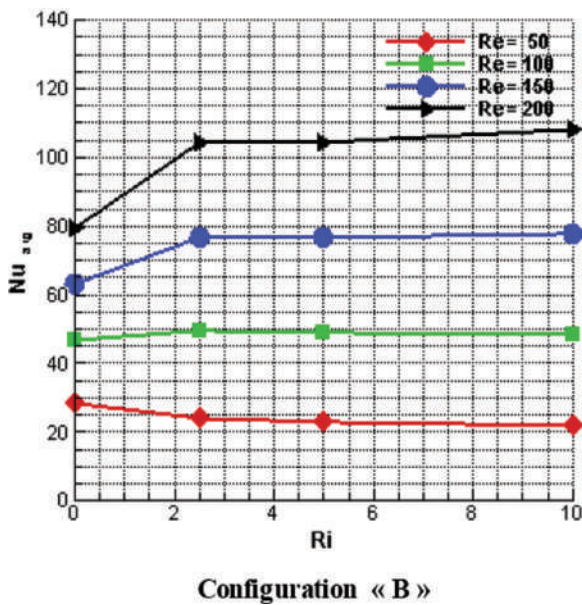
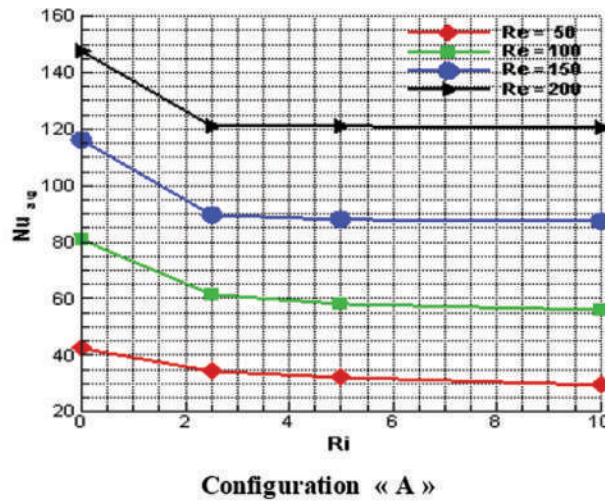


Figure 10. The average Nusselt number as a function of the Richardson number for different Reynolds numbers with amplitude of and phase-deviation of the three configurations.

presented in Figure 9 in the case of forced convection the isotherms are concentrated vertically near the hot source and as the number of Re increases, a stratification of the isotherms at the top of the cavity for low values of Re the transfer by conduction is dominant than the convection. On the other hand, the more Ri increases, the isotherms are narrowed and they are concentrated around the source since the transfer by convection is dominant than the conduction and the more Re increases which induces a rapid flow speed of the fluid.

Heat transfer rate

A variation of the mean Nusselt number as a function of the Richardson number for different Reynolds numbers on

the hot wall of the cavity of the three configurations studied above is represented in the Figure 10. We notice, through the profile of the configuration “C” where the position of the source located at the bottom and to the left of the cavity. The average Nusselt number increases from Ri = 0 to Ri = 2.5 and vice versa for the case of the “A” configuration where the position is at the top right of the cavity. Then it remains almost constant beyond this value for the set of Re values of the two cases. On the other hand, in the case of the configuration “B” where the position is in the center, the average Nusselt number is almost constant as a function of Ri for different numbers of Re. Nevertheless, by comparing quantitatively the value of the transfer rate is larger in configuration “A” this is due to the increase in

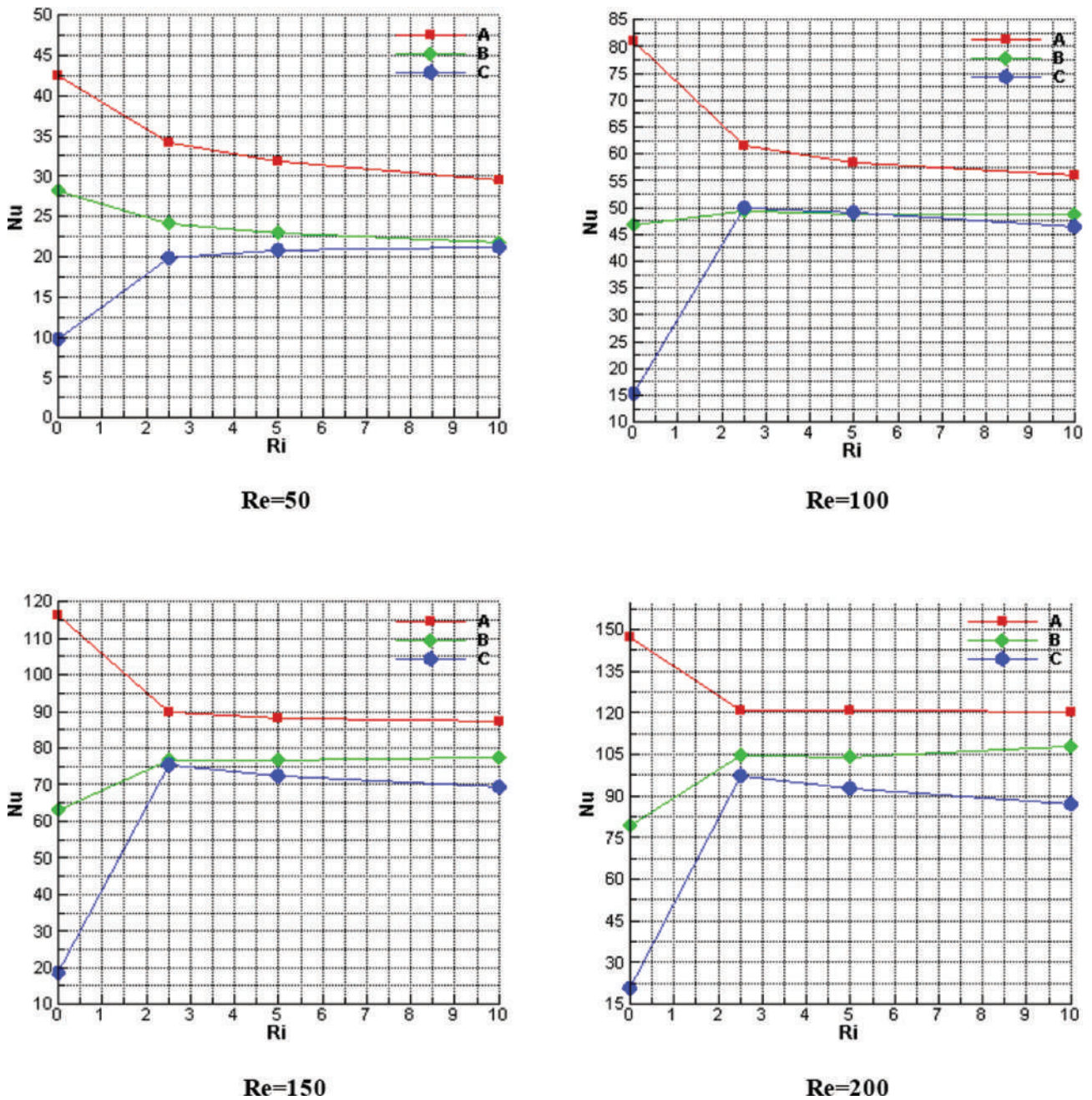
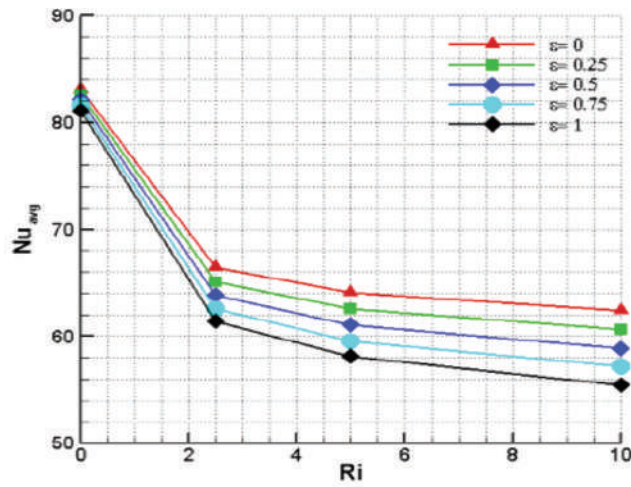


Figure 11. The variation of the mean Nusselt number as a function of the Richardson number of the three configurations for each Reynolds number.

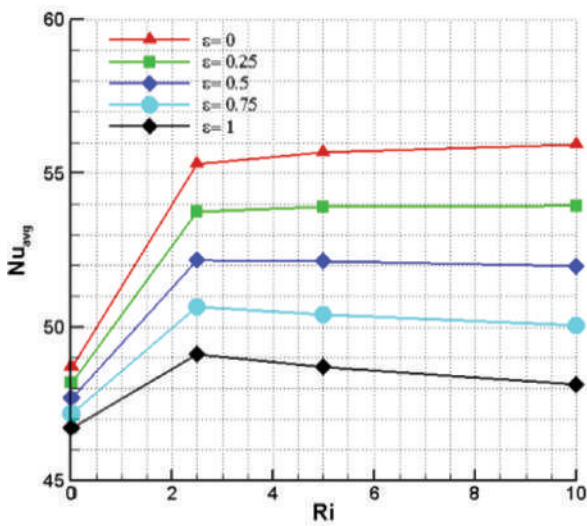
convective effects and consequently to the intensification of heat exchanges between the heat source and the flowing fluid. Note that the positioning of the heat source at the top near the right vertical wall of the cavity gives a better heat transfer rate, especially for high values of the Reynolds number.

The Figure 11 shows the variation of the average Nusselt number as a function of the Richardson number of the three configurations for each Reynolds number, we notice that the Nusselt number decreases by increasing the Richardson

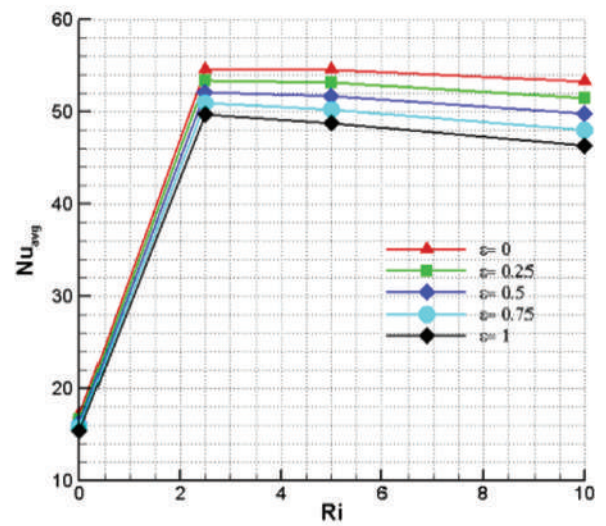
number whatever Re for the configuration “A “. But we see in the configuration “C” the Nu increases in the phase of forced convection $Ri = 0$ to 2.5 then it decreases by increasing the Re. On the other hand, the configuration “B” the heat transfer rate registers a stability except for the phase of the low numbers of Ri where it experiences a decrease, then it increases with the large values of Re. The significant increase in average Nusselt number for low Ri values corresponds to a dominant forced convection in configuration « C ».



Configuration « A »



Configuration « B »



Configuration « C »

Figure 12. The Nusselt number profile as a function of the Richardson number for different values of the sinusoidal temperature amplitude $\epsilon = 1$ for the three configurations.

Effect of the amplitude and phase-deviation:

Figure 12 illustrates the Nusselt number profile as a function of the Richardson number for different values of the amplitude of the sinusoidal temperature imposed on the right vertical wall of the three configurations studied. The Nu decreases in the case of the source is positioned at the top of the right side (configuration “A”) then it becomes constant where the position of the source is in the center (configuration “B”) and the Nu increases in the case of the source is located at the bottom left side (“C” configuration). However, the average heat transfer

rate increases with decreasing excitation temperature amplitude in the three cases of configurations studied. So conversely that we vary the frequency of the imposed temperature, we recorded that the average heat transfer rate of the air increases with the increase in the frequency of the temperature. This implies that heat transfer by convection is more dominant than transfer by conduction regardless of the magnitude or frequency of the imposed temperature. But quantitatively, increasing the amplitude and frequency respectfully decreases and increases the transfer rate.

CONCLUSION

A digital scan of a rectangular cavity has an inlet and an outlet of air containing a heated solid body studied at three different positions. The right vertical wall is heated by a temperature of the sinusoidal shape and the other wall subjected to a cold temperature. The top and bottom of the cavity remain without heat exchange with the external environment. The study leads to the following conclusions:

- As Ri increases, convection strengthens with primary vortices, in half of the cavity and conduction becomes prominent in the vicinity of the solid body and the wall in the “A” configuration. while the “B” configuration, exhibits strong convective movement adjoining the two zones located in the vicinity of the hot source which in turn stretches the primary vortices outward through the orifice in the right-side wall. In the “C” configuration, the appearance of two counter-rotating recirculation zones with strong convection in the cell located between the solid body and the right-side wall.
- Heat transfer by convection is dominant over conduction, increasing the Richardson number with increasing Reynolds number.
- The transfer rate increases with the decrease in the amplitude of the excitatory temperature. On the other hand, it decreases with the increase in the frequency of the sinusoidal temperature.

The mean temperature of the fluid and the Nusselt number on the right wall and the square solid depend strongly on:

- Entry and exit positions;
- Dimension and position of the solid block.

NOMENCLATURE

| | |
|-----|---|
| H | Cavity height, m |
| L | Cavity Length, m |
| d | Solid block side length |
| Pr | Prandtl number |
| Re | Reynolds number |
| Ri | Richardson number |
| Gr | Grashof number |
| g | Gravitational acceleration, m.s-2 |
| Nu | Average Nusselt number along the heat wall |
| w | Height of the opening (m) |
| u,v | Dimensional velocity components (ms-1) |
| U,V | Dimensionless velocity components along X and Y, respectively |
| x,y | Cartesian coordinates, m |
| X,Y | Dimensionless coordinate |
| p | Pressure, kPa |
| P | Dimensionless pressure |
| T | Dimensional temperature (K) |
| q | Heat source at solid boundaries |

h Convective heat transfer coefficient

Greek symbols

| | |
|---------------|---|
| α | Thermal diffusivity, m ² . s-1 |
| β | Thermal expansion coefficient, K-1 |
| Θ | Dimensionless temperature |
| μ | Dynamic viscosity, kg. m-1.s-1 |
| ρ | Density, kg.m-2 |
| ϕ | Phase deviation |
| ε | Amplitude ratio |
| λ | Thermal conductivity |
| ν | Kinematic viscosity, m ² .s |

Subscripts

| | |
|-----|-------------|
| avg | Average |
| f | Fluid |
| s | Solid |
| i | Inlet state |
| h | Hot |
| c | Cold |

AUTHORSHIP CONTRIBUTIONS

Authors equally contributed to this work.

DATA AVAILABILITY STATEMENT

The authors confirm that the data that supports the findings of this study are available within the article. Raw data that support the finding of this study are available from the corresponding author, upon reasonable request.

CONFLICT OF INTEREST

The author declared no potential conflicts of interest with respect to the research, authorship, and/or publication of this article.

ETHICS

There are no ethical issues with the publication of this manuscript.

REFERENCES

- [1] Moraga NO, López SE. Numerical simulation of three-dimensional mixed convection in an air-cooled cavity. *Numer Heat Transf Part A Appl* 2004;45:811–824. [\[CrossRef\]](#)
- [2] Aminossadati SM, Ghasemi B. A numerical study of mixed convection in a horizontal channel with a discrete heat source in an open cavity. *Eur J Mech B/Fluids* 2009;28:590–598. [\[CrossRef\]](#)

- [3] Carozza A. Numerical study on mixed convection in ventilated cavities with different aspect ratios. 2018;3:11. [\[CrossRef\]](#)
- [4] Douha M, Belkacem D, Noureddine K, Houari A, Abdellah B, Elmir M, et al. Study of laminar naturel convection in partially porous cavity in the presence of nanofluids. *J Adv Res Fluid Mech Therm Sci* 2021;79:91–110. [\[CrossRef\]](#)
- [5] Rahman MM, Alim MA, Saha S, Chowdhury MK. Effect of the presence of a heat conducting horizontal square block on mixed convection inside a vented square cavity. *Nonlinear Anal Model Control* 2009;14:531–548. [\[CrossRef\]](#)
- [6] Rahman MM, Alim MA., Mamun MAH. Finite element analysis of mixed convection in a rectangular cavity with a heat-conducting horizontal circular cylinder. *Nonlinear Anal Model Control* 2009;14:217–247. [\[CrossRef\]](#)
- [7] Noghrehabadi A, Ghalambaz M, Izadpanahi E, Pourrajab R. Effect of magnetic field on the boundary layer flow, heat, and mass transfer of nanofluids over a stretching cylinder. *J Heat Mass Transf Res* 2014;1:9–16. [\[CrossRef\]](#)
- [8] Yahiaoui K, Nehari D, Draoui B. The investigation of the mixed convection from a confined rotating circular cylinder. *Period Polytech Mech Eng* 2017;61:161–172. [\[CrossRef\]](#)
- [9] Yuce BE, Pulat E. Forced, natural and mixed convection benchmark studies for indoor thermal environments. *Int Commun Heat Mass Transf* 2018;92:1–14. [\[CrossRef\]](#)
- [10] Abbassi MA, Djebali R, Guedri K. Effects of heater dimensions on nanofluid natural convection in a heated incinerator shaped cavity containing a heated block. *J Therm Eng* 2018;4:2018–2036. [\[CrossRef\]](#)
- [11] Revnic C, Ghalambaz M, Groşan, Şheremet M, Pop I. Impacts of non-uniform border temperature variations on time-dependent nanofluid free convection within a trapezium: Buongiorno's nanofluid model. *Energies* 2019;12:1461. [\[CrossRef\]](#)
- [12] Ali MM, Alim MAA, Ahmed SS. Finite element solution of hydromagnetic mixed convection in a nanofluid filled vented grooved channel. *J Therm Eng* 2020;7:91–108. [\[CrossRef\]](#)
- [13] Selimefendigil F, Öztöp HF. Mixed convection in a single-walled carbon nanotube-water nanofluid filled partially heated triangular lid-driven cavity having an elastic bottom wall. *J Therm Eng* 2020;6:379–387. [\[CrossRef\]](#)
- [14] Mohammed AA. Natural convection heat transfer inside horizontal circular enclosure with triangular cylinder at different angles of inclination. *J Therm Eng* 2021;7:240–254. [\[CrossRef\]](#)
- [15] Saha S, Mamun AH, Hossein MZ, Sadr Aleslam AKM. Mixed convection in an enclosure with different inlet and exit configurations. *J Appl Fluid Mech* 2008;01:78–93.
- [16] Mekroussi S, Kherris S, Mebarki B, Benchatti A. Mixed convection in complicated cavity with non-uniform heating on both sidewalls. *Int J Heat Technol* 2017;35:1023–1033. [\[CrossRef\]](#)
- [17] Manca O, Nardini S, Khanafer K, Vafai K. Effect of heated wall position on mixed convection in a channel with an open cavity. *Numer Heat Transfer A* 2003;43:259–282. [\[CrossRef\]](#)
- [18] Chamkha AJ, Hussain SH, Abd-Amer QR. Mixed convection heat transfer of air inside a square vented cavity with a heated horizontal square cylinder. *Numer Heat Transf Part A Appl* 2011;59:58–79. [\[CrossRef\]](#)
- [19] Rahman MM, Alim MA, Saha S., Chowdhury MK. A numerical study of mixed convection in a square cavity with a heat conducting square cylinder at different locations. *J Mech Eng* 2008;39:78–85. [\[CrossRef\]](#)
- [20] Rahman M, Alim MA, Saha S, Chowdhury M.K. Mixed convection in a vented square cavity with a heat conducting horizontal solid circular cylinder. *J Nav Archit Mar Eng* 2008;5:37–46. [\[CrossRef\]](#)
- [21] Karimi F, Xu H, Wang Z, Yang M, Zhang Y. Numerical simulation of steady mixed convection around two heated circular cylinders in a square enclosure. *Heat Transf Eng* 2016;37:64–75. [\[CrossRef\]](#)
- [22] Rahman M, Alim MA, Arif M, Mamun H. “Numerical study of opposing mixed convection in a vented enclosure. *ARNP J Eng Appl Sci* 2007;2:25–36.
- [23] Ibrahim W, Hirpho M. Finite element analysis of mixed convection flow in a trapezoidal cavity with non-uniform temperature. *Heliyon* 2021;7:e05933. [\[CrossRef\]](#)
- [24] Sivasankaran S, Sivakumar V, and Prakash P. Numerical study on mixed convection in a lid-driven cavity with non-uniform heating on both sidewalls. *Int J Heat Mass Transf* 2010;53:4304–4315. [\[CrossRef\]](#)
- [25] Saha S, Islam MT, Ali M, Mamun MAH, Islam MQ. Effect of inlet and outlet locations on transverse mixed convection inside a vented enclosure. *J Mech Eng* 1970;36:27–37. [\[CrossRef\]](#)
- [26] Doghmi H, Abourida B, Belarache L, Sannad M, Ouzauit M. Numerical study of mixed convection inside a three-dimensional ventilated cavity in the presence of an isothermal heating block. *Int J Heat Technol* 2018;36:447–456. [\[CrossRef\]](#)
- [27] Dechaumphai P. Finite Element Method in Engineering. Bangkok: Chulalongkorn University Press, 1999.
- [28] Taylor C, Hood P. A numerical solution of the Navier-Stokes equations using the finite element technique. *Comput Fluids* 1973;1:73–100. [\[CrossRef\]](#)